Applications of Element Overlay Technique to the Problems of Particulate Composite Materials

H. Okada[1], C. T. Liu[2], T. Ninomiya[1], Y. Fukui[1], N. Kumazawa[1]

Summary

In this paper, an extension of element overlay technique (s-FEM) [1] for particulate composite material (see [2], for example) to perform three-dimensional elastic-plastic analysis is presented. Mathematical formulations that allows us to generate meso-scale analysis models for particulate composite materials is first presented. We adopt an incremental formulation for elastic-plastic analysis. We then present a numerical example.

Introduction

In this paper, an element overlay technique is applied to the problems of particulate composite materials. Element overlay technique was first present by Fish [3] as s-version FEM (s-FEM) and then adopted by researchers to solve various problems [4,5,6].

In the applications of the element overlay technique, an analysis model is generated by superposing two kinds of finite element models. One is called "global model" and the other is "local model", in this paper. Global model represents the structure or representative volume as whole. Local model is for the localized structural details such as distributed reinforcing particles/fibers, as shown in Fig. 1. When the shapes of the distributed reinforcing particles/fibers are the same, we can use the same local model repeatedly. In other words, the local model is generated once and is superposed on the global model repeatedly. Present authors applied such a technique to the two-dimensional analyses of particulate composite materials [1].

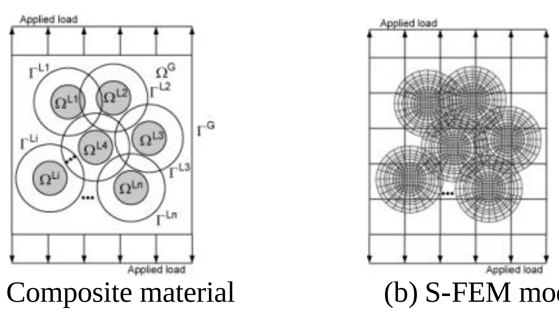

(a) Composite material (b) S-FEM model

Fig. 1 Composite material and its s-FEM model.

[1] Kagoshima University, Kagoshima University, Kagoshima, Japan

[2] Air Force Research Laboratory, Edwards AFB, CA, USA

In this paper, the method presented in [1] is extended to deal with three-dimensional elastic-plastic problems. Mathematical formulations are briefly presented first and some issues in numerical treatments in three-dimensional elastic-plastic problems are described.

Mathematical Formulations

Second phase materials (particles or fibers) or voids distribute in matrix material, as shown in Fig. 1. They are modeled by overlaid finite element meshes, whose regions are denoted by Ω^{Li} $(i=1,2,3,\cdots,n)$. We call them as "Local Mesh Regions". The global structure is modeled by a coarse finite element mesh within Ω^G. We call this region as "Global Mesh Region". In present work, the local mesh regions are contained within Ω^G. Each local mesh region contains only one particle, fiver or void. We allow the local mesh regions to overlap each other.

We denote the displacement increments to be Δu_i^G and Δu_i^{Li} $(i=1,2,3,\cdots,n)$ that are based on the shape functions of the global and the local meshes in Ω^G and Ω^{Li}. The displacement functions are superposed when the global and the local mesh regions overlap each other. For example, for a region, where the global and the local mesh regions (Ω^{Lp}, Ω^{Lq} and Ω^{Lr}) overlap, we write the displacement increments Δu_i, as:

$$\Delta u_i = \Delta u_i^G + \Delta u_i^{Lp} + \Delta u_i^{Lq} + \Delta u_i^{Lr} \tag{1}$$

At a point, where any local mesh regions do not overlap with the global mesh region, the displacements u_i equal u_i^G ($u_i = u_i^G$). The continuities of the displacements are enforced by letting the functions u_i^{L1}, u_i^{L2}, u_i^{L3}, $\cdots$, u_i^{Ln} be zero at the outer boundaries Γ^{Li} of the local mesh regions Ω^{Li}. The statement of principle of virtual work in an incremental formulation is written to be:

$$\int_{\Omega^G} \frac{\partial \Delta du_i}{\partial x_j} D^{ep}_{ijk\ell} \frac{\partial \Delta u_k}{\partial x_\ell} \mathrm{d}\Omega^G = \int_{\Gamma_t^G} d\Delta u_i \Delta \bar{t}_i \mathrm{d}\Gamma_t^G \tag{2}$$

where the variations of the displacements are defined in the same manner as the displacements. Γ_t^G denotes the boundary where the tractions $\bar{t}_i$ are prescribed. $E_{ijk\ell}$ are the forth order tensor representing material's stress-strain relationship (incremental J2-flow elastic-plastic constitutive law.). We then substitute the displacements and their variations in the statement of principle of virtual work. After some algebraic manipulations, we have:

$$\int_{\Omega^G} \frac{\partial \Delta du_i^G}{\partial x_j} D^{ep}_{ijk\ell} \frac{\partial \Delta u_k^G}{\partial x_\ell} \mathrm{d}\Omega^G + \sum_{q=1}^{n} \int_{\Omega^{L1}} \frac{\partial \Delta du_i^G}{\partial x_j} D^{ep}_{ijk\ell} \frac{\partial \Delta u_k^{Lq}}{\partial x_\ell} \mathrm{d}\Omega^{Lq} = \int_{\Gamma_t^G} du_i \Delta \bar{t}_i \mathrm{d}\Gamma_t^G \tag{3}$$

$$\begin{aligned}&\int_{\Omega^{Lp}} \frac{\partial \Delta du_i^{Lp}}{\partial x_j} D_{ijk\ell}^{ep} \frac{\partial \Delta u_k^{G}}{\partial x_\ell} \mathrm{d}\Omega^{Lp} + \int_{\Omega^{Lp}} \frac{\partial \Delta du_i^{Lp}}{\partial x_j} D_{ijk\ell}^{ep} \frac{\partial \Delta u_k^{Lp}}{\partial x_\ell} \mathrm{d}\Omega^{Lp} \\ &+ \sum_{\substack{q=1 \\ q\neq p}}^{n} \int_{\Omega^{Lp-Lq}} \frac{\partial \Delta du_i^{Lq}}{\partial x_j} D_{ijk\ell}^{ep} \frac{\partial \Delta u_k^{Lq}}{\partial x_\ell} \mathrm{d}\Omega^{Lp-Lq} = 0 \qquad (p = 1,2,3,\cdots,n)\end{aligned} \tag{4}$$

It is noted here that the left hand side of equation (4) equals zero, since the local mesh regions do not intersect with the outer boundary of the structure. Ω^{Lp-Lq} ($p,q = 1,2,3,\cdots,n;\ p \neq q$) denote regions sheared by Ω^{Lp} and Ω^{Lq} (i.e., $\Omega^{Lp-Lq} = \Omega^{Lp} \cap \Omega^{Lq}$). When $0 = \Omega^{Lp} \cap \Omega^{Lq}$, the related terms in equation (4) disappear. After the global and local regions are discretized by appropriate finite elements, we can write a matrix formulation, as:

$$\begin{bmatrix} \boldsymbol{K}^{G} & \boldsymbol{K}^{G-L1} & \boldsymbol{K}^{G-L2} & \cdots & \boldsymbol{K}^{G-Ln} \\ \boldsymbol{K}^{L1-G} & \boldsymbol{K}^{L1} & \boldsymbol{K}^{L1-L2} & \cdots & \boldsymbol{K}^{L1-Ln} \\ \boldsymbol{K}^{L2-G} & \boldsymbol{K}^{L2-L1} & \boldsymbol{K}^{L2} & \cdots & \boldsymbol{K}^{L2-Ln} \\ \vdots & \vdots & \vdots & \ddots & \vdots \\ \boldsymbol{K}^{Ln-G} & \boldsymbol{K}^{Ln-L1} & \boldsymbol{K}^{Ln-L2} & \cdots & \boldsymbol{K}^{Ln} \end{bmatrix} \begin{Bmatrix} \Delta \boldsymbol{u}^{G} \\ \Delta \boldsymbol{u}^{L1} \\ \Delta \boldsymbol{u}^{L2} \\ \vdots \\ \Delta \boldsymbol{u}^{Ln} \end{Bmatrix} = \begin{Bmatrix} \Delta \boldsymbol{f}^{G} \\ \boldsymbol{0} \\ \boldsymbol{0} \\ \vdots \\ \boldsymbol{0} \end{Bmatrix} \tag{5}$$

where $\Delta \boldsymbol{u}^{G}$ and $\Delta \boldsymbol{u}^{Lp}$ are the column vectors of unknown nodal displacements of the global and the local meshes. Matrices $\boldsymbol{K}^{G}$, $\boldsymbol{K}^{Lp}$, $\boldsymbol{K}^{G-Lp}$, $\boldsymbol{K}^{Lp-Lq}$ arise from the integrals in the left hand sides of equations (3) and (4). Since, $\boldsymbol{K}^{G-Lp} = \left(\boldsymbol{K}^{Lp-G}\right)^{T}$ and $\boldsymbol{K}^{Lp-Lq} = \left(\boldsymbol{K}^{Lq-Lp}\right)^{T}$, the global stiffness matrix in the right hand side of equation (8) is symmetric. However, the global stiffness matrix is not banded, unlike an ordinary finite element method. $\Delta \boldsymbol{f}^{G}$ is the consistent nodal force vector arising from the right hand side of equation (3).

Solution procedures

The coefficient matrix of equation (5) is symmetric and positive definite. However, the coefficient matrix looses a band structure, as there are many off-diagonal components. In such a case, use of iterative equation solver is advantageous over direct solvers. Thus, we adopted an Incomplete Cholesky-decomposition-preconditioned conjugate gradient (ICCG) method [7].

In present study, a mid-point radial return algorithm (Atluri [8]) is employed for time integration of stresses. Incremental elastic-plastic analysis is carried out without iterative solution procedures.

Numerical treatments for coupling stiffness matrix

When the coupling stiffness matrices such as $\boldsymbol{K}^{Lp-G}$, $\boldsymbol{K}^{Lp-Lq}$, etc. are evaluated, numerical integrals are performed. For example, when the coupling stiffness matrix $\boldsymbol{k}^{Lpi-Lqj}$ between the *i*-th element of local mesh region *p* and *j*-th element of local mesh region *q*, computed, an integral as shown below is performed.

$$\boldsymbol{k}^{Lpi-Lqj} = \int_{\Omega^{Lpi}} a^{Lpi-Lqj}(\boldsymbol{x})\left(\boldsymbol{B}^{Lpi}\right)^T \boldsymbol{D}^{ep}\boldsymbol{B}^{Lqj}\mathrm{d}\Omega^{Lpi} \tag{6}$$

where $\boldsymbol{B}^{Lpi}$ and $\boldsymbol{B}^{Lqj}$ are the strain-displacement matrix for the elements, and $\boldsymbol{D}^{ep}$ is the matrix representing the incremental tangent stiffness. Ω^{Lpi} is the volume of the *i*th element of local mesh region *p*. Integration is performed based on Ω^{Lpi}. It is however noted that the integration may be performed on Ω^{Lpj}. $a^{Lpi-Lqj}(\boldsymbol{x})$ is a scalar function whose value is "1" or "0". At a point, where Ω^{Lpi} and Ω^{Lpj} overlaps, the value of $a^{Lpi-Lqj}(\boldsymbol{x})$ is "1". Otherwise, $a^{Lpi-Lqj}(\boldsymbol{x})$ is "0". Therefore, the integrand of eq. (6) may have some discontinuities within the volume Ω^{Lpi}. An ordinary Gauss quadrature would fail to evaluate the integral accurately.

For example, as shown in Figure 2 (a), Ω^{Lpi} and Ω^{Lpj} partially overlap each other, and the integration is performed based on Ω^{Lpi}. First, Ω^{Lpi} is divided into 8 sub-cells. Then each subdivided-cell is checked if it intersects with the faces of Ω^{Lpj}. If a subdivided-cell intersects with the faces of Ω^{Lpj}, it is divided into 8 sub-cells again. This process is repeated until the smallest sub-cell becomes small enough (typically within 1% of Ω^{Lpi}). The processes of creating sub-cells are shown in Figs. 2 (b)~(d). Then, an ordinary Gauss quadrature rule is applied in each subdivided-cell.

Numerical example

As an example problem, a block that contains 9 spherical particles is considered. The volume fraction of voids/particles is 6.51%. The model is shown in Figure 3.

In Figure 4, the distribution of equivalent stress normalized by yield stress for a section intersecting four particles is depicted for the stage of elastic deformation. It is seen that stress in the particles is higher than in matrix material. Particles are connected through the region of high stress. The distributions of equivalent plastic strain and equivalent stress are depicted in Figures 5 and 6, when the block is subject to 2% of tensile strain. Plastic strain is accumulated at the top and bottom of the particles, as seen in Figure 5. In Figure 6, the distribution of equivalent stress normalized by yield stress is depicted the regions of high stress running vertically and connect the particles. Figures 5 and 6 clearly indicate the effects of particle interaction.

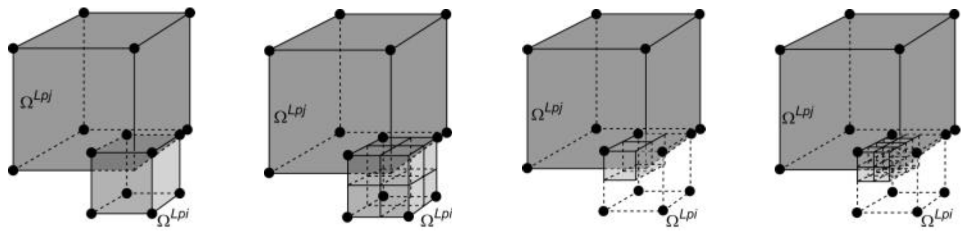

(a) (b) (c) (d)

Figure 2 Elements Ω^{Lpi} and Ω^{Lpj} partially overlapping each other and the generation of subdivisions for numerical integration [(a) Elements Ω^{Lpi} and Ω^{Lpj} partially overlapping, (b) Element Ω^{Lpi} divided by eight sub-cells, (c) Sub-cells of Ω^{Lpi} that do not overlap with element Ω^{Lpj} deleted, (d) Each sub-cells of Ω^{Lpi} is divided into eight sub-cells.].

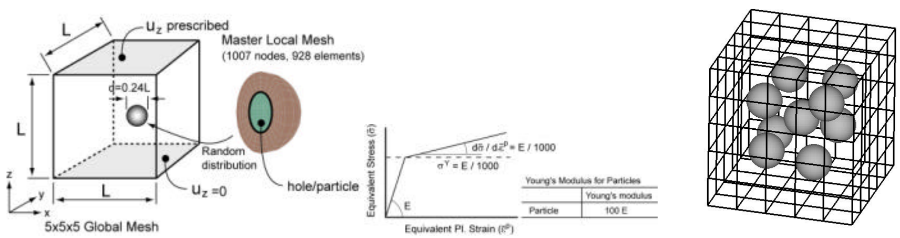

Figure 3 Nine spherical void/particle problem for elastic-plastic analysis.

Concluding Remarks

In this paper, the element overlay technique for the meso-mechanics analysis of particulate composite material is presented. The formulation allows to perform incremental nonlinear analysis. The interaction between reinforcing particles can be investigated using present methodology.

Acknowledgement

Present investigation has been supported by AOARD. The authors would like to express sincere gratitude to Dr. K. Goretta of AOARD.

Reference

1 Okada, H., Ninomiya, T. Sakasegawa, Y., Fukui, Y., Kumazawa, N. (2003): "Macro/Meso Mechanics Analyses for Composite Materials by using an Element Overlay Technique", *ICCES'03 (CDROM)*, Eds. Atluri, S.N., et al.

2 Kwon, Y. W., Liu, C. T. (2003): "Microstructural Effects on Damage Behavior in Particulate Reinforced Composites", *Polymer & Polymer Composites*, Vol. 11, pp. 1-8.

3 Fish, J. (1992): "The s-Version Finite Element Method", *Computers & Structures*, Vol. 43, pp. 539-347.

4 Fish, J. and Guttal, R. (1996): "The s-Version of Finite Element Method for Laminated Composites", *Int. J. Numer. Methods Eng.*, Vol. 39, pp. 3641-3662.

5 Nakasumi, S., Suzuki, K., Fujii, D., Ohtsubo, H. (2003): "Mixed Analysis of Shell and Solid Elements using the Overlaying Mesh Method", *J. Mar. Sci. Technol.*, Vol. 7, pp. 180-188.

6 Okada, H., Endoh, S., Kikuchi, M. (2004): "On Fracture Analysis using an Element Overlay Technique", *Key Engineering Materials*, Vols. 261-263, pp. 681-686.

7 Oguni, C., Murata, T., Miyoshi, T., Dongarra, J.J. and Hasegawa, H. (1993): *Gyoretu Keisan Software (in Japanese, Software for Matrix Calculations)*, Maruzen, Tokyo.

8 Atluri, S.N. (1985): "Notes and Comments on Computational Elastoplasticity: Some New Models and Their Numerical Implementation", *Proc. Int. Conf. Finite Elements in Computational Mechanics*, pp. 271-289.

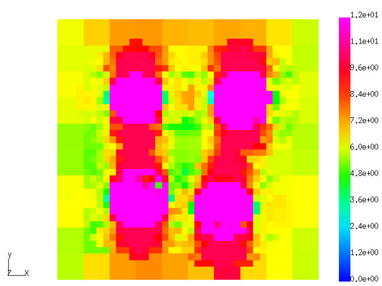

Figure 4 Distributions of equivalent stress before any plastic deformation takes place.

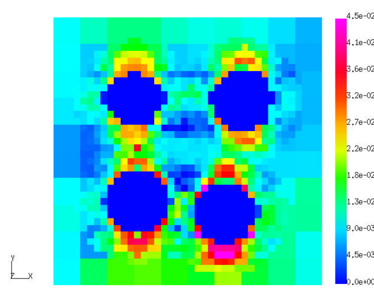

Figure 5 Distribution of equivalent plastic strain for the problem of nine spherical particles.

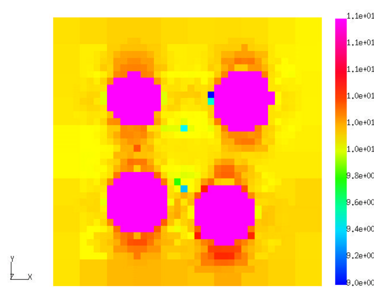

Figure 6 Distribution of equivalent stress strain after some plastic deformation, for the problem of nine spherical voids/particles.